

Mécanismes moléculaires
impliqués dans la réduction
des mortalités
d'huîtres creuses causées par
OsHV-1 à 29°C.

- *Présentation de l'article 2 (in prep)*

Le travail présenté dans le chapitre précédent montre que le maintien des huîtres à 29°C pendant leur infection par OsHV-1 augmente significativement leur survie sans altérer ni l'infectivité du virus ni sa virulence. Après 14 jours, les huîtres infectées maintenues à 29°C présentaient une survie de 85,7%, tandis que les témoins d'infection maintenus à 21°C affichaient une survie de 52,4%. Aux deux températures, l'ADN et l'ARN d'OsHV-1 ont été détectés. Cependant la réplication virale d'OsHV-1 et le taux d'ADN viral ont été réduits significativement chez des huîtres maintenues à 29°C (Delisle et al., 2018b).

On sait que la température module profondément la physiologie des organismes marins en régulant la vitesse des réactions chimiques et enzymatiques, les vitesses de diffusion, la fluidité membranaire et la structure des protéines (Hochachka et Somero, 2002). Des études antérieures ont montré que le stress thermique induisait l'expression de gènes liés au système immunitaire chez les huîtres (Green et al., 2014; Zhang et al., 2015), cependant, son effet sur la capacité de réponse de l'huître aux agents pathogènes reste flou.

Le travail présenté dans ce second article vise à étudier les mécanismes physiologiques responsables de l'augmentation de la survie et de la réduction de la réplication virale à 29°C. Pour ce faire, à partir des échantillonnages réalisés dans l'expérience 1A (décrits dans le chapitre précédent), nous avons analysé les transcriptomes des huîtres infectées à 29°C et à 21°C dès les premières heures de cohabitation. Quatre temps d'analyses ont été choisis : 0, 12, 24 et 48 heures post-cohabitation afin d'étudier la réponse immédiate de l'hôte à l'infection et d'identifier les mécanismes biologiques différenciant les animaux infectés à 29°C de ceux infectés à 21°C. Des analyses lipidiques et biochimiques complémentaires ont été réalisées afin d'évaluer la modulation thermique de la composition des membranes, des réserves énergétiques et de l'activité de quelques enzymes, pour tenter de définir leur potentielle implication dans l'amélioration de la survie des huîtres.

High temperature induces transcriptomic changes in *Crassostrea gigas* that hinders progress of Ostreid herpes virus (OsHV-1) and promotes survival.

Lizenn Delisle^{1*}, Marianna Pauletto², Bruno Petton¹, Luca Bargelloni², Fabrice Pernet¹,
Elodie Fleury¹ and Charlotte Corporeau¹.

¹ Ifremer, UMR 6539 CNRS/UBO/IRD/Ifremer, Laboratoire des sciences de l'Environnement Marin (LEMAR), 29280 Plouzané, France.

² Department of Comparative Biomedicine and Food Science. University of Padova, Viale dell'Università 16, 35020 Legnaro, Padova, Italy.

* **Corresponding author:** Charlotte Corporeau, Centre Ifremer de Bretagne, CS 10070, 29280 Plouzané, France. Tél: +33 2 98 22 43 86. Fax: + 33 2 98 22 46 53. E-mail: Charlotte.Corporeau@ifremer.fr

Background

Mortality outbreaks in Pacific oyster *Crassostrea gigas* associated with infection by viral and bacterial pathogens have increased during the last 10 years worldwide (Barbosa Solomieu et al., 2015; EFSA, 2010; Pernet et al., 2016). The most striking example is the massive mortality of less than one-year old individuals, which can decimate up to 100% of the farmed oysters during the warm season. These mortalities coincided with the recurrent detection of ostreid herpesvirus 1 (OsHV-1) variants (Jenkins et al., 2013; Lynch et al., 2012; Mortensen et al., 2016; Segarra et al., 2010). The virus creates an immune-compromised state of oysters evolving towards subsequent bacteremia by opportunistic bacterial pathogens leading to oyster death (de Lorgeril et al., 2018). Concomitantly, like other herpesviruses, OsHV-1 uses the host cell machinery to replicate (Jouaux et al., 2013; Renault and Novoa, 2004; Segarra et al., 2014b) and alter its metabolism (Corporeau et al., 2014; Pernet et al., 2018, 2014b; Tamayo et al., 2014; Young et al., 2017).

Seawater temperature is a major trigger of marine disease by influencing the host and the pathogen (Burge et al., 2014; Harvell et al., 2002). Temperature modulate physiology of the host by altering velocity of chemical and enzymatic reactions, rates of diffusion, membrane fluidity and protein structure (Hochachka and Somero, 2002; Pernet et al., 2007). Previous

studies showed that thermal stress induces the expression of important immune-related genes in oysters, possibly affecting host response to OsHV-1 (Green et al., 2014a; Zhang et al., 2015a). In experimentally infected shrimp, the overexpression of heat shock protein 70 (hsp70) mRNA by a non-lethal heat shock induced a significant reduction of the gill-associated virus (GAV) and the white spot syndrome virus (WSSV) replication (De La Vega et al., 2006; Lin et al., 2011).

Regarding OsHV-1, the optimal seawater temperature in Europe for disease transmission and subsequent mortalities is between 16°C and 24°C (Pernet et al., 2012; Renault et al., 2014). In a previous paper, we found that survival of oysters challenged with OsHV-1 at 29°C was markedly higher (85.7%) than at 21°C (52.4%) whereas virus infectivity and virulence were unaltered (Delisle et al., 2018b). We therefore hypothesize that differences in survival between temperature reflect a host response to the pathogen. To test this hypothesis, we characterized at the physiological condition of oysters at 21°C and 29°C and then compared their transcriptomes during the course of infection. In contrast to previous studies which describes the mechanisms of infection under permissive conditions by comparing healthy vs. infected (Jouaux et al., 2013; Rosani et al., 2015a) or resistant vs. susceptible populations (de Lorgeril et al., 2018; Segarra et al., 2014b), we investigate the physiological mechanisms that modulate the severity of the disease by infecting susceptible oysters at two temperatures that are more or less permissive.

Results

We first characterized the initial physiological condition of oysters at 21°C and 29°C by means of biochemical analyses. Proximate composition (protein, lipid and carbohydrate) and citrate synthase activity of oysters acclimated at 21°C and 29°C were remarkably similar (Table S1). In contrast, unsaturation index of polar lipids, an indicator of thermal adaptation of biological membranes, was higher at 21°C than at 29°C, mostly reflecting variations in 20:5n-3. Finally, the ratio of the fatty acids 20:4n-6 to 20:5n-3 increased with temperature.

We then investigated the temporal transcriptomic response of oysters at 21°C and 29°C using 0 hpc as a reference point for each temperature. We found that the number of differentially abundant (DA) transcripts increased from 38 to 1413 between 12 and 48 hpc in oysters at 21°C while it remained low in oysters at 29°C (39 and 271 at 12 and 48 hpc respectively, Figure 1).

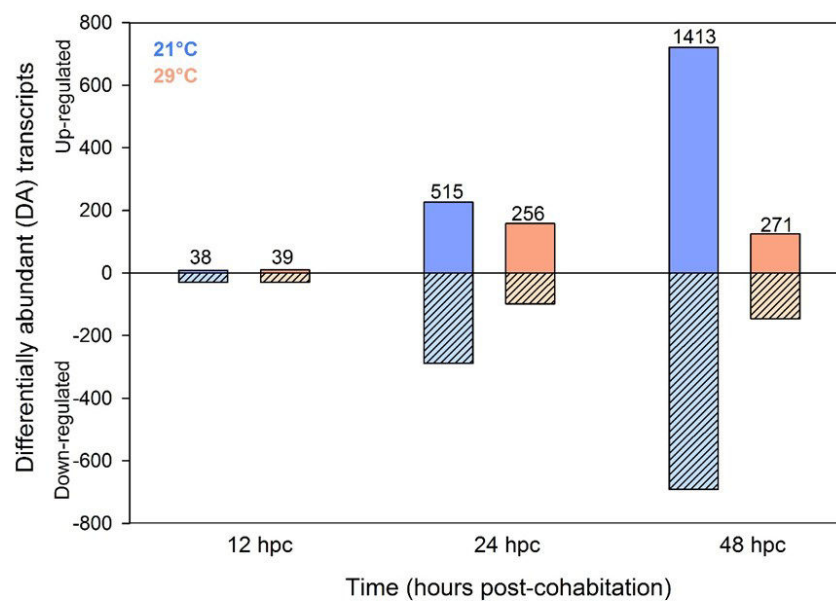


Figure 1. Number of differentially abundant (DA) transcripts in oysters infected at 21°C and 29°C 12, 24 and 48 h post-cohabitation (hpc) compared to 0 hpc (reference). The total number of DA transcripts is indicated above each bar.

At 21°C 12 hpc, gene ontology revealed that DA transcripts were associated to 9 biological processes (BP) that were all related to innate immune response (Table S2). Then, at 24 hpc, the most enriched BPs among the 515 DA transcripts were related to antiviral immunity (Table S3). Moreover, BPs linked to macromolecules synthesis, organization of cellular matrix and developmental processes were markedly enriched (Table S3). Concomitantly, BPs related to negative regulation of necrosis, cell death, protein maturation, and inhibition of G2/M transition of mitotic cell cycle were enriched (Table S3). At 48 hpc, transcripts related to innate immune response remained abundant (Table S4). Transcripts related to negative regulation of cell death and negative regulation of protein maturation processes were over-abundant, while those related to growth; metabolic processes and regulation of cardiac muscle contraction were less-abundant (Table S4).

At 29°C 12 hpc, DA transcripts were associated to 19 BPs related to innate immune response (Table S2). At 24 hpc, the depleted BPs were related to growth processes and cell development, and transmembrane transport (Table S3). The most depleted BP was the “regulation of

endoplasmic-reticulum-associated protein degradation pathway” (Table S3). Besides, transcripts coding apoptotic processes such as “lymphocyte apoptotic process”, “regulation of extrinsic apoptotic signaling pathway” and “cell death” were less abundant. Low abundance of transcripts involved in metabolic processes persisted 48 hpc. Transcripts linked to “system process”, “endothelial cell development”, “regulation of anatomical structure morphogenesis”, “divalent metal ion transport” were less abundant, whereas those related to innate immunity, “defense response to virus” and “cellular homeostasis” were over-abundant (Table S4).

We then compared the transcriptome of oysters infected at 29°C and 21°C (reference) at each time point to identify factors required for the repression of infection at 29°C (Figure 2). We found that oyster transcriptomes at 29°C and 21°C were similar before infection as only 9 DA transcripts came out. However, the number of DA transcripts increased to 1400 at 12 hpc and decreased to 289 and 92 at 24 and 48 hpc respectively. Therefore, the effect of temperature on the transcriptomic response of infected oysters was particularly strong 12 hpc and we focused the functional enrichment analysis on this point.

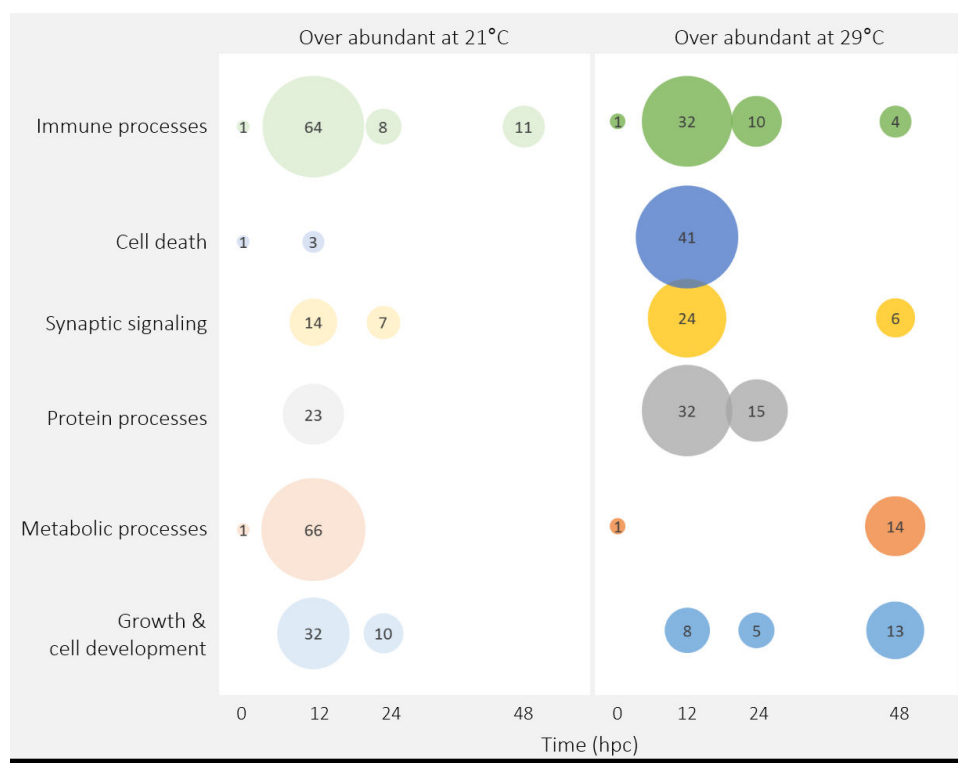


Figure 2. Number of differentially abundant (DA) transcripts per functional categories, in oysters infected at 29°C 0, 12, 24 and 48 h post-cohabitation compared to their counterparts infected at 21°C.

The functional enrichment analysis revealed that the number of DA related to immunity was 64 at 21°C and 32 at 29°C (Figure 3). These transcripts coded for immune receptors (pattern recognition receptors, immune receptor lectins, immune receptor FBG domain containing), intracellular immune signaling proteins (interleukins, cytokines, and growth factors), and for effector genes involved in cytolytic pathways or complement pathways were over-abundant at 21°C (Figure 3). However, transcripts coding for immune receptor LRR containing protein, intracellular transduction TLR adaptor molecules, and immune receptor pattern recognition receptors like scavenger receptor cysteine-rich repeat protein, RIG-I like receptor, NACHT and leucine-rich repeat receptors were more abundant at 29°C than at 21°C.

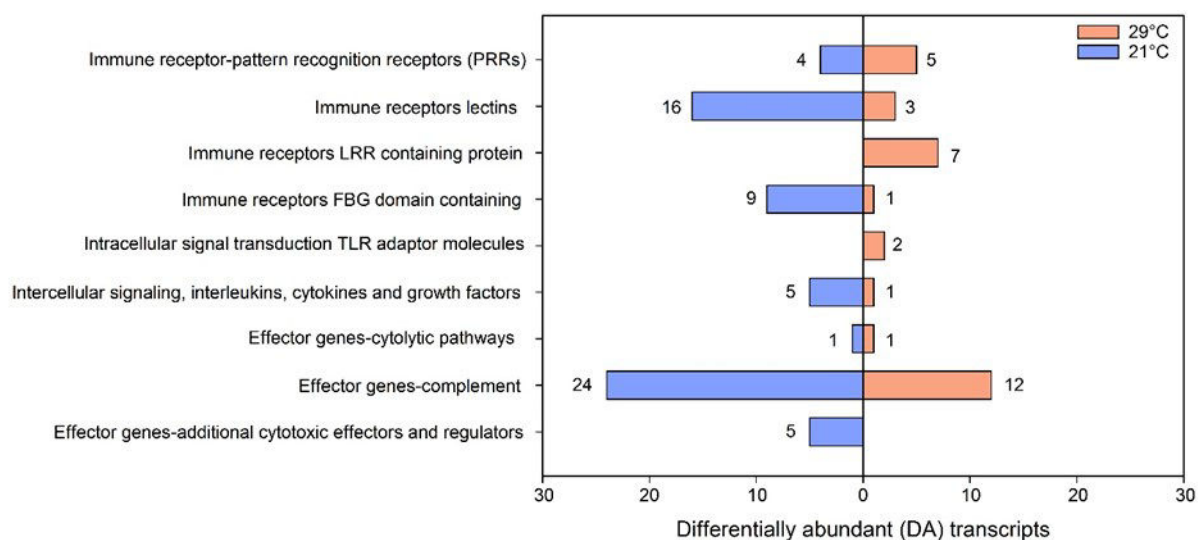


Figure 3. Number of differentially abundant (DA) transcripts related to immune processes in oysters infected at 29°C 12 h post-cohabitation compared to their counterparts infected at 21°C.

The functional enrichment analysis also showed that transcripts related to cell death, synaptic signaling, and protein processes were more abundant in oysters at 29°C than at 21°C whereas it was the inverse for those related to metabolism, and growth and cell development (Figure 2).

Over-abundant transcripts at 29°C related to cell death coded for 11 proteins involved in cell death *per se*, one autophagy protein and five apoptosis inhibitor proteins (Table S5). Those related to synaptic signaling coded for neurotransmitter synaptic receptors such as acetylcholine, GABA, glycine, serotonin, thyrotropin releasing hormone, and members of glutamate pathway, neuropeptide receptor and G protein subunit alpha (Table S6). Finally,

over-abundant transcripts at 29°C related to protein process coded for ubiquitin conjugating enzyme E2, E3 ubiquitin ligases proteins in charge of the substrate specificity (24 DA transcripts), and 3 deubiquitinase proteins were identified as regulators of this process (Table S7). Transcripts E3 are involved in regulation of apoptosis, protein translation arrest via EIF4E2 ubiquitination, degradation of misfolded proteins, regulation of immune response and major histocompatibility complex (MHC).

Over-abundant transcripts at 21°C related to metabolic processes coded for several proteins involved in catabolism of carbohydrate (4), amino acid (5) and triglyceride (4) and synthesis of fatty acids and phospholipid (3) and amino-acids (3) (Table S8). Transcripts coding for proteins involved in energy production pathways such as glycolysis (5), neoglucogenesis (1), penthose-phosphate (4), and transport of monocarboxylate metabolites (5) were also more abundant at 21°C than at 29°C. Finally, some over-abundant transcripts at 21°C were also related to cholesterol metabolic process (5), retinol metabolism (5), and transcription/translation processes (11).

Over-abundant transcripts at 21°C were also associated to processes like “regulation of growth”, and “cell adhesion”. These transcripts coded regulators of tissue growth (MEGF10, NOTCH1, CD63 antigen), and particularly for extracellular matrix components (Collagen alpha chain, Chondroitin Sulfate Proteoglycan, Uromodulin, Table S9). Interestingly, the chondroitin sulfate proteoglycan was strongly down-expressed at 29°C like five members of the Tetraspanin family, likely reflecting that these transcripts are associated to proteins that are involved in the entry of OsHV-1 in host cell. Other transcripts were involved in cell-cell adhesion (SVEP 1, contracted associated protein, Neurexin-2-alpha), wounding repairs and inflammatory responses (Thrombospondin-1 and 2, Tenascin, and Ninjurin-1). Most of these genes are associated to membrane glycoproteins that regulate numerous cellular functions such as cell extracellular matrix attachment, immunity, and cell migration.

Discussion

In a previous paper, we found that survival of oysters challenged with OsHV-1 at 29°C was markedly higher than at 21°C whereas virus infectivity and virulence were unaltered (Delisle et al., 2018b). Here we investigate how temperature influenced the host response to the pathogen by comparing transcriptomes (RNA-sequencing) during the course of infection at 21°C and 29°C. We found temperature influenced immune processes, cell death, synaptic

signaling, protein processes, metabolism and growth and cell development (Figures 2). These processes occur in all stages of infection and are summarized in Figure 4.

Prior to infection, oysters at 21°C and 29°C showed only 9 differentially abundant (DA) transcripts, suggesting that they were fully acclimated. This is consistent with the fact that filtration rates of oysters (Delisle et al., 2018b) and their proximate composition and aerobic metabolism (citrate synthase activity) were similar between temperature. Also, the unsaturation index of polar lipids, an indicator of thermal adaptation of biological membranes, varied consistently with temperature (Hochachka and Somero, 2002; Pernet et al., 2007).

The number of DA transcripts varied from 9 to 1415 depending on temperature and time. In previous studies investigating the response of oysters to OsHV-1 infection, the number of DA transcripts varied from 250 to 9400 (de Lorgeril et al., 2018; Jouaux et al., 2013; Rosani et al., 2015a). The relatively low number of DA transcripts obtained here probably reflects that we compared transcriptomes of susceptible and infected oysters at two temperatures which exhibited subtle differences in disease severity. Although survival was markedly different between temperature treatments, levels of OsHV-1 DNA in oysters at 21°C and 29°C reached the same maximum values 24-48 h after the onset of infection (Delisle et al., 2018b).

The number of DA transcripts in oysters infected at 21°C increased markedly throughout the duration of the study whereas it remained low and stable at 29°C. Similar differences in the number of DA transcripts were reported when comparing transcriptomes of oyster families with contrasted resistance phenotypes with regards to the disease (de Lorgeril et al., 2018). For instance, the number of DA transcripts increases markedly during the time course of infection in susceptible oyster family whereas it remains low and stable in resistant family (de Lorgeril et al., 2018). Therefore, from a quantitative point of view, the temporal RNA response of oysters infected at 21°C and 29°C resemble that of susceptible and resistant families respectively.

Our results suggest that seawater temperature could modulate the entry of OsHV-1 into the host cell by modulating the composition of the cell matrix and the attachment of the virus in a way consistent with a reduced susceptibility of the host to the virus at 29°C. For instance, transcripts coding for chondroitin sulfate proteoglycans (CSPGs) were much less abundant at 29°C than at 21°C 12 hpc. This protein is a major component of the extracellular matrix of vertebrates, which, among other things, participates in the attachment of the herpes simplex virus 1 to the host cell (Mårdberg et al., 2002). In *C gigas*, CSPGs are particularly abundant in gills (Zhang

et al., 2012), which is the portal of entry of pathogens like OsHV-1 (Martenot et al., 2016; Segarra et al., 2015). Previous studies suggested that heparan sulfate, another extracellular matrix component, could be implicated in OsHV-1 entry in oysters cells (Jouaux et al., 2013; Segarra et al., 2014b). We also found that five members of Tetraspanins, a family of transmembrane proteins, were less abundant at 29°C. Among these proteins, the CD63 transcripts which code for an antigen involved in the entry of several types of viruses into host cells (Spoden et al., 2008; Van Spriel and Figdor, 2010).

Our results suggest that temperature modulated oyster immunity. For instance, transcripts related to immune receptor LRR containing protein, intracellular transduction Toll like Receptor adaptor molecules, and some immune receptor pattern recognition receptors, like scavenger receptor cysteine-rich repeat protein, RIG-I like receptor, NACHT and leucine-rich repeat receptors were more abundant in oysters at 29°C than at 21°C. Temperature naturally increases the abundance of transcripts related to immunity such as Toll like receptors, RIG-I, and Tumor necrosis factors in healthy oysters (Meistertzheim et al., 2007; Zhang et al., 2015a). Interestingly, transcripts coding for Toll like receptors pathway and RIG-I like receptor are activated in oyster during OsHV-1 replication (de Lorgeril et al., 2018; Green and Montagnani, 2013; He et al., 2015; Huvet et al., 2004; Rosani and Venier, 2017; Zhang et al., 2011). Although scavenger receptors, NACHT and leucine-rich repeat receptors have not been reported in previous transcriptional studies of oysters, these proteins can recognize viral nucleotides and participate in induction of anti-viral mediators in vertebrates (DeWitte-Orr et al., 2010; Martinez et al., 2011; Takeuchi and Akira, 2007).

In support to the transcriptomic results, the ratio of the fatty acids 20:4n-6 to 20:5n-3 increased with temperature, suggesting that the immune status of oysters was more favorable at 29°C. Indeed, these two fatty acids are involved in eicosanoid production which are associated with stimulation of immune function in invertebrates (Howard and Stanley, 1999). However, eicosanoids produced from 20:4n-6 are generally more active than those produced from 20:5n-3, and the replacement of 20:5n-3 by 20:4n-6 in bivalves decreases immune parameters of hemocytes (Delaporte, 2003; Delaporte et al., 2007, 2006).

We found that temperature increased the abundance of pro-apoptotic transcripts in oysters 12 hpc. Apoptosis is one of the major mechanisms of antiviral response inducing the abortion of viral multiplication and the elimination of viral progeny by premature lysis of infected cells (Pilder et al., 1984). Therefore, over-abundance of some pro-apoptotic transcripts at 29°C may

have limited virus proliferation, as previously reported in shrimps exposed to high temperature treatment during a viral infection (Granja et al., 2003). In the same time, some transcripts coding for inhibitors of apoptosis were also over-abundant at both 21°C and 29°C. The role of apoptosis during OsHV-1 infection is still unclear (de Lorgeril et al., 2018; Rosani et al., 2015a; Segarra et al., 2014b; Wang et al., 2018).

Temperature also influenced the ubiquitylation/proteasome system of oysters. For instance, the number of DA transcripts coding for the ubiquitylation/proteasome system were more abundant at 29°C 12 hpc. Similarly, number of DA transcripts related to ubiquitylation process increased during the first 6-12 h post-infection and were higher in resistant than in susceptible oysters (de Lorgeril et al., 2018). Moreover, the amount of protein related to ubiquitination process were altered in infected oysters (Corporeau et al., 2014). In vertebrates, ubiquitylation and proteolysis are involved in protein recycling and regulate the stability, activity and localization of target proteins (Bhoj and Chen, 2009). Several over-abundant transcripts identified in our study belong to protein E3 which is involved in major histocompatibility complex, apoptosis, cell cycle and the protein translation arrest. These processes are crucial for mounting an adequate immune response and more probably to fight against bacterial pathogens (Cheng et al., 2016; Seo et al., 2013). It is therefore likely that over-stimulation of the proteasome system in oysters at 29°C could limit the bacteremia that normally follow OsHV-1 infection (de Lorgeril et al., 2018).

We found that transcripts related to several neurotransmitter synaptic receptors were over-abundant in oysters infected at 29°C 12 hpc. These transcripts coded for receptors for acetylcholine, GABA, glutamate, serotonin, thyrotropin-releasing hormone, and gonadotropin-releasing hormone. Oyster hemocytes generally have receptors for several neurotransmitters that are previously listed. Hemocytes regulate receptors abundance during immune response to influence apoptosis and phagocytosis, indicating that, once the host recognized an invader, some neurotransmitters might be released to optimize immune responses (Li et al., 2016; Liu et al., 2017). In oysters, the release of GABA and acetylcholine seems to be activated by immune stimulation and they tend to down-regulate the immune response at long-time scale, avoiding the excess immune reactions to maintaining the immune homeostasis (Li et al., 2016; Liu et al., 2017; Wang et al., 2018). At 29°C, over-expression of neuroendocrine receptors could optimize immune activities helping to eliminate OsHV-1 and to restore homeostasis after viral elimination.

In response to viral infection at 29°C, transcripts related to catabolism, metabolites transport, amino acids, nucleotides and fatty acids synthesis, transcription, and translation were less abundant at 29°C than at 21°C. This probably reflects that OsHV-1, like other herpesvirus, alter host cell metabolic pathways to provide an optimal environment for its replication and spread (De la Re Vega et al., 2017). More particularly, viruses increase *i*) nucleotide synthesis to supply rapid viral genome replication, *ii*) amino acid production used for virion assembly, *iii*) lipid availability to provide additional membrane material for envelopment of viral particles and *iv*) ATP flux for supporting the energy cost of genome replication and packaging (Sanchez and Lagunoff, 2015; Yu et al., 2011). More specifically, OsHV-1 increases glycolysis, TCA cycle, and fatty acid synthesis and triglyceride catabolism (Corporeau et al., 2014; Young et al., 2017). Other studies report depletions of host carbohydrate and triglyceride reserves during OsHV-1 infection (Pernet et al., 2018, 2014b; Tamayo et al., 2014). Here we showed that hijacking of the host cell machinery by OsHV-1 was altered at 29°C.

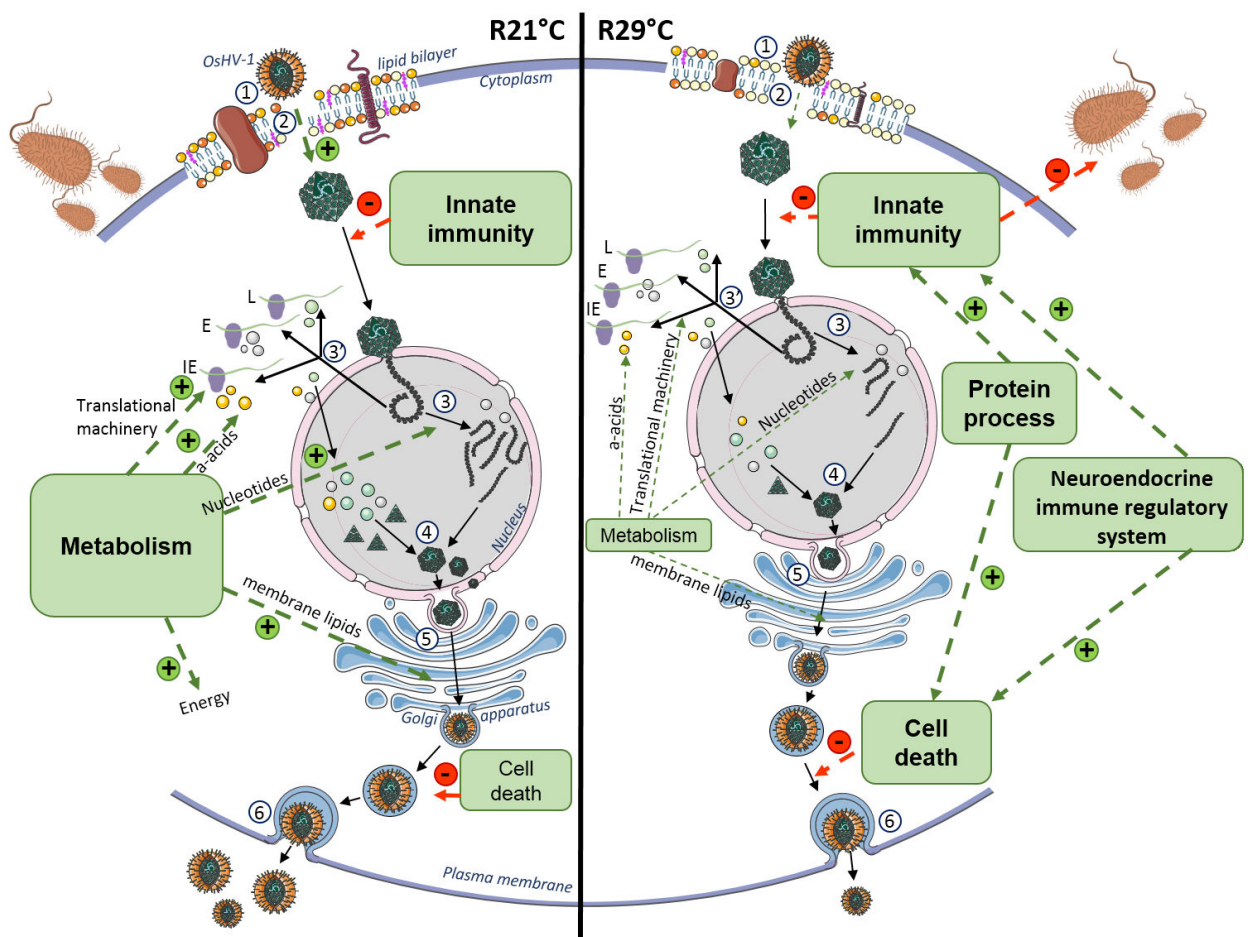
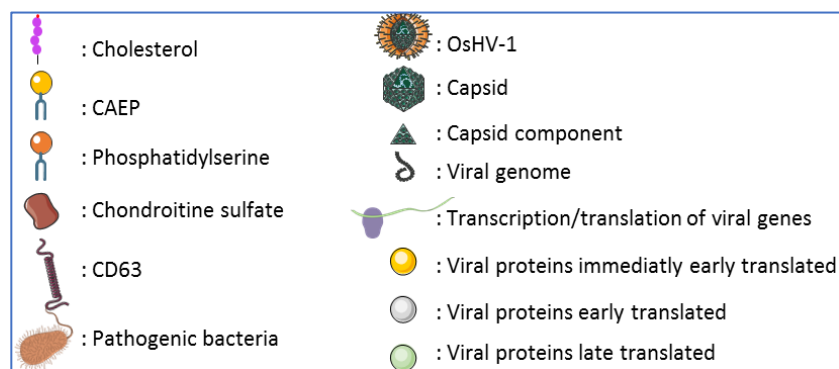


Figure 4. Schematic presentation of physiological responses occurring in oysters infected at 29°C and 21°C 12 hpc. This picture is a data compilation of our study and the life cycle of

OsHV-1 proposed by (Jouaux et al., 2013). Font size increase for upregulated processes and decrease for those that were down-regulated. The green + and the red - arrows indicate the positive and negative effect of each process on oyster disease. Numbers refer to the different steps of *OsHV-1* cycle: 1: viral attachment, 2: membranes fusion, 3: viral genome replication, 3': transcription and translation of viral DNA, 4: capsid assembly, 5: envelopment of viral particle and releasing of mature virion. Abbreviations: IE, viral genes that are expressed immediately early after the onset of infection; E refers to genes that are expressed early, and L to genes expressed late (Jouaux et al., 2013; Segarra et al., 2014a).



Methods

Experimental design

Details about the rearing procedures and experimental design are presented in a previous paper (Delisle et al., 2018b). Briefly, specific pathogen-free oysters were produced in hatchery at the Ifremer facilities in Argenton according to (Petton et al., 2015a). Prior to starting the experiments, young oysters were maintained in 500L open flow tank under controlled conditions (21°C, 35.2‰ salinity, O₂ > 85%), and fed *ad libitum*. At the onset of the experiment, oysters were 8 months old with a mean weight of 1.48 g. On 9 May 2016, oysters were divided in two groups, oysters for injection with a suspension of *OsHV-1* (*i.e.* pathogen donors) or oysters for cohabitation with pathogen donors (*i.e.* pathogen recipients). Pathogen donors were left at 21°C (control temperature) in 500L tank while recipient oysters were transferred in 45L tanks either left at 21°C or gradually increase to 29°C at 2°C day⁻¹ (n=3 replicate tanks per temperature). On 19 May, oysters for injection were myorelaxed in MgCl₂ and injected with 100 µl of viral suspension containing 6.9×10^6 copies of *OsHV-1* µVar in the adductor muscle, and incubated at 21°C during 5 hours. Then, injected oysters (now pathogen donors) were transferred into the 45L tanks to cohabit with the recipients acclimated at 21°C or

29°C. Survival of recipients was followed every day for 14 days (Delisle et al. 2018), and 15 recipients per tank were sampled at 0, 12, 24, 48 hours post cohabitation (hpc). Whole oyster tissues were removed from the shell, frozen in liquid nitrogen and individually ground in liquid nitrogen with a MM400 homogenizer (Retsch, Eragny, France). One individual oyster per tank was used for transcriptomic analyses and one pool of nine oysters was used for biochemical analysis (n=3 replicate tank for each temperature).

RNA extraction and RNA sequencing

A total of 45 libraries were sequenced corresponding to 3 individuals exposed to OsHV-1 (N=3) à 21°C or 29°C (2 temperatures) and sampled at 0 hpc, 12 hpc, 24 hpc, and 48 hpc (4 times).

Reads processing

Initial quality control was carried out with the FastaQC software (<http://www.bioinformatics.babraham.ac.uk/projects/fastqc/>) version 0.11.5 (Andrews, 2010). In order to filter out any remaining post-sequencing ribosomal RNA, the local sequence alignment tool SortMeRna 2.0 (Kopylova et al., 2012) was applied against different public databases (Rfam 5.8S; Rfam 5S; Silva 16S archaeal, bacterial; Silva 18S eukaryote; Silva 23S archaeal, bacterial; Silva 28S eukaryote) and a custom database including *C. gigas* ribosomal RNAs. Raw reads were then trimmed for low quality bases using CLC Genomics Workbench v 11.0 as follows: 1) Illumina adapters were removed; 2) only reads with less than 2 ambiguous nucleotides were allowed; 3) reads with >5% nucleotide with PHRED scores <20 were filtered out; 4) broken pairs were discarded.

Reads mapping

Reads were mapped against the Ensembl *C. gigas* reference genome v 9.38 by means of the STAR aligner and following the two-pass mapping mode (Dobin and Gingeras, 2015). The maximum number of mismatches allowed was set to 20 and only uniquely mapped reads were counted. Read counts for each sample, at the gene level, were extracted by setting the “GeneCounts” quantification while running STAR.

Differential expression analysis

The read counts obtained from the STAR aligner were used for the differential gene expression analysis conducted using the Bioconductor package edgeR version 3.10.0 (Robinson et al., 2010) in the R environment (version 3.2.2). Samples were grouped according to condition, temperature and time. The edgeR “calcNormFactors” normalization function was used to find a set of scaling factors for the library sizes that minimized the log-fold changes between samples. The scale factors were computed using a trimmed mean of M-values (TMM) between samples (Robinson et al., 2010). After estimating dispersions, the glmLRT test provided in edgeR was used to assess differentially abundant transcripts (DA) between experimental conditions, with a threshold for a significant false discovery rate (FDR) set to < 0.05 .

Functional enrichment

A functional interpretation of the lists of significant genes was obtained through enrichment analysis using the Database for Annotation, Visualization, and Integrated Discovery (DAVID) software. “Biological process” (BP) annotation categories (BP_FAT) were used by setting the gene count equal to 3 and the *e*-value equal to 0.05. Since the DAVID database contains functional annotation data for a limited number of species, it was necessary to link the *C. gigas* genes with sequence identifiers that could be recognized in DAVID. This process was accomplished using Uniprot/Swiss-prot accession IDs corresponding to each contig. These identifiers were used to define a “gene list” of DA transcripts and a “background” in the bioinformatic tool DAVID.

Biochemical analysis

Lipid class determination

Lipid class determination was obtained using 300 mg homogenized in 6 ml chloroform-methanol (2:1, v/v) according to Folch, (Folch et al., 1957). Neutral and polar lipid class determination were performed using a CAMAG automatic sampler (CAMAG, Switzerland) as described in Da Costa et al., 2016. These methods allowed to separate the different lipid classes such as sterols (ST), alcohols (AL), alkenones 1 and 2 (ALK 1 and 2), free fatty acids (FFA), triacylglycerol (TAG), glyceryl ethers (GE) and sterol esters (StE) for neutral lipids and lysophosphatidyl-choline (LPC), sphingomyelin (Sm), phosphatidylcholine (PC),

phosphatidylserine (PS), phosphatidylinositol (PI), phosphatidylethanolamine (PE) and cardiolipin (Ca) for phospholipids.

Fatty acid composition

Fatty acid composition was analyzed in neutral and polar lipids of oysters infected at 21°C or 29°C at 0 hpc, 12 hpc, 24 hpc and 48 hpc. Neutral and polar lipids were separated using a silica gel micro-column as described in Marty and collaborators (Marty et al., 1992). Each lipid fraction was transesterified (Metcalf and Schmitz, 1961) and analyzed in a gas chromatograph with an on-column injector, DB-Wax capillary column and a flame ionization detector. Fatty acids were then identified by comparison of retention times with standards.

Carbohydrates

Samples of 50 mg of powder were homogenized in 2 ml of nanopure water using a Polytron® PT 2500 E (Kinematica, Luzernerstrasse, Switzerland) and diluted 10 times. Carbohydrate concentrations were determined by colorimetric method according to (DuBois et al., 1956). Samples (250 µl) were mixed with phenol (0.5 ml, 5% m/v), and incubated for 20 min. Sulfuric acid (2.5 ml, 96 %) was added in samples. Absorbance was read at 490 nm and at 600 nm with a UV 941 spectrophotometer (Kontron instruments, San Diego, California, USA). Carbohydrates concentrations were determined with the following formula: $[Abs = ABS_{490nm} - 1.5 \times (ABS_{600nm} - 0.003)]$ and using a standard calibration curve. Concentration was expressed as mg of carbohydrates per g of dry weight.

Proteins and Citrate synthase activity

Total protein extraction was performed as describe in (Delisle et al., 2018a) using 600mg of recipient oysters powder. Total protein concentration of each lysate was determined using the DC protein assay (Bio-Rad). The resulting lysates were divided in aliquots and stored at -80°C until enzymatic assays.

All the assays were performed in triplicate at room temperature. Enzyme activity were measured using Nunc TM 96-well microplates (Thermo Scientific), a synergy HT microplate reader and the software Gen5, both from Biotek (Winooski, Vermont, USA). Enzymatic activity was measured and related to the total protein concentration of each sample.

Enzymatic activity of citrate synthase (CS; EC 2.3.3.1) was measured using 20 μ L of total protein lysates as describe in (Epelboin et al., 2015; Fuhrmann et al., 2018).

Supplementary data

Table S1: Proximate composition, citrate synthase activity, fatty acids composition in polar lipids and unsaturation index of oysters at 0 hpc, acclimated since 10d at 21°C or 29°C.

	21°C	29°C
Proximate composition		
Protein (% dry weight)	36.2 \pm 5	34.2 \pm 4.6
Carbohydrates (% dry weight)	10.3 \pm 2.4	13.1 \pm 0.5
Triglycerides (μ g.mg ⁻¹)	3.4 \pm 0.7	4.5 \pm 0.9
Enzyme assay		
Citrate synthase (mU.mg protein ⁻¹)	47.9 \pm 6.6	49.1 \pm 8
Fatty acids composition (%) in polar lipids		
14:0	1.9 \pm 0.1	2.1 \pm 0.1
16:0	12 \pm 0.5	13.4 \pm 0.5
18:0 dma	7.8 \pm 0.9	7.9 \pm 0.6
18:00	3.1 \pm 0.1	2.9 \pm 0.2
18:1n-7	7.4 \pm 0.3	7.5 \pm 0.2
20_1n-11	1.8 \pm 0.2	2.7 \pm 0.4
20:1n-7	4.6 \pm 0	4.6 \pm 0.3
20:4n-6	5.5 \pm 0.2	6.4 \pm 0.4
20:5n-3	14.2 \pm 0.6	11.3 \pm 0.7
22:6n-3	13.7 \pm 0.3	13.1 \pm 0.2
22:2 NMI	6.2 \pm 0.4	6 \pm 0.8
20:4/20:5	0.38 \pm 0.0	0.57 \pm 0.1
Unsaturation index	245.8 \pm 3.5	236.4 \pm 0.8

Table S2, S3, S4

These supplementary data are available online. They correspond to gene enrichment analysis performed on the transcriptomic response of oysters at 21°C and 29°C using 0 hpc as a reference point for each temperature

<https://drive.google.com/open?id=1sfja6qVTbZ9mEK489BzEg1LLJrOemZ9EB>

Table S5. Transcripts related to cell death process differentially expressed at 12 hpc.

Biological process	Gene name	CGI	LFC	P-value
Cell death	MAP3K	CGI_10003652	3.09	<0.001
	Caspase-2	CGI_10014678	1.02	0.007
	Growth arrest-specific protein 2	CGI_10006013	2.18	0.004
	Pericentrin	CGI_10001236	2.20	0.002
	Heme-binding protein 2	CGI_10011388	2.11	<0.001
	Programmed cell death protein 10	CGI_10002438	2.91	0.002
	Programmed cell death protein 4	CGI_10028820	2.46	0.002
	Ubiquitin carboxyl-terminal hydrolase 27	CGI_10005873	1.81	<0.001
	X-box-binding protein 1	CGI_10005445	1.17	0.002
	Metalloproteinase inhibitor 3	CGI_10000389	1.75	<0.001
	Multiple epidermal growth factor-like domains 10	CGI_10014528	2.03	0.006
Autophagy	Autophagy protein 5	CGI_10018604	1.93	<0.001
Cell death inhibitor	HCLS1-associated protein X-1-like	CGI_10011394	1.51	<0.001
	Apoptosis 1 inhibitor	CGI_10026772	4.43	<0.001
	Heat shock protein beta-1	CGI_10011376	2.16	<0.001
	Inhibitor of apoptosis protein	CGI_10005393	4.41	0.003
	Putative inhibitor of apoptosis	CGI_10019869	1.49	0.008

Table S5: Changes in the transcriptional expression of the *C. gigas* apoptosis related genes of R29°C compared to R21°C transcriptomic response, during the early response to OsHV-1 infection. (LFC: Log Fold Change)

Table S6. Transcripts related to cell synaptic signaling differentially expressed at 12 hpc.

Biological process	Gene name	CGI	LFC	P-value
Acetylcholine	Acetylcholine receptor subunit alpha-like 2	CGI_10021702	2.47	<0.001
GABA	Gamma-aminobutyric acid type B receptor ssu 2	CGI_10018562	3.80	0.004
Glutamate	Glutamate receptor 4	CGI_10015550	1.07	0.004
	Glutamate receptor, ionotropic kainate 2	CGI_10006846	2.32	0.043
	Vesicular glutamate transporter 2	CGI_10023398	1.31	<0.001
	Metabotropic glutamate receptor 5	CGI_10011484	1.44	<0.001
	Protein lin-10	CGI_10017177	2.64	0.002
Glycine	Glycine receptor subunit alphaZ1	CGI_10008177	1.76	0.006
Serotonin	5-hydroxytryptamine receptor 1A-alpha	CGI_10008776	1.82	0.003
	5-hydroxytryptamine receptor 2A	CGI_10012065	1.54	0.004
Prot G transduction	G protein subunit alpha	CGI_10012977	2.82	<0.001
TRH	Thyrotropin-releasing hormone receptor	CGI_10023293	1.78	<0.001
Neuropeptide	Gonadotropin-releasing hormone II receptor	CGI_10022302	1.52	0.005
Regulators	Alsin	CGI_10012236	1.81	<0.001

Table S6: Changes in the transcriptional expression of the *C. gigas* synaptic signaling related genes of R29°C compared to R21°C transcriptomic response, during the early response to OsHV-1 infection (LFC: Log Fold Change).

Table S7. Transcripts related to protein process differentially expressed at 12 hpc.

Biological process	Gene name	CGI	LFC	P-value
E2	Ubiquitin-conjugating enzyme E2 Q1-like	CGI_10025987	3.61	<0.001
	Ubiquitin-conjugating enzyme E2 U	CGI_10008530	1.81	0.001
	Ubiquitin-conjugating enzyme E2-17 kDa	CGI_10015505	0.96	0.009
E3	E3 ubiquitin-protein ligase rnf213-alpha	CGI_10005453	1.78	0.005
	Ariadne-1-like protein	CGI_10024285	2.09	<0.001
	DCN1-like protein 4	CGI_10003817	2.82	0.004
	E3 ubiquitin-protein ligase DZIP3	CGI_10018771	1.44	0.005
	E3 ubiquitin-protein ligase MIB1	CGI_10026035	1.27	0.009
	Inhibitor of apoptosis protein	CGI_10005393	4.41	0.003
	Protein deltex-3-like protein	CGI_10002382	1.86	0.005
	Putative E3 ubiquitin-protein ligase ARI3	CGI_10023357	1.64	<0.001
	Putative E3 ubiquitin-protein ligase HECTD3	CGI_10028530	1.51	0.003
	Putative inhibitor of apoptosis	CGI_10007421	1.49	0.008
	Transcription intermediary factor 1-beta	CGI_10003254	3.33	0.002
	Tripartite motif-containing protein 2	CGI_10006172	2.08	<0.001
	Tripartite motif-containing protein 2	CGI_10013768	2.71	<0.001
	Tripartite motif-containing protein 2	CGI_10001580	2.09	0.006
	Tripartite motif-containing protein 2	CGI_10005584	1.89	0.002
	Tripartite motif-containing protein 2	CGI_10003706	2.39	0.002
	Tripartite motif-containing protein 2	CGI_10017589	2.49	<0.001
	Tripartite motif-containing protein 2	CGI_10020024	1.78	<0.001
	Tripartite motif-containing protein 2	CGI_10013767	1.16	0.008
	Tripartite motif-containing protein 2	CGI_10019703	2.91	<0.001
	Tripartite motif-containing protein 2	CGI_10022495	1.61	0.002
	Apoptosis 1 inhibitor	CGI_10021439	4.43	<0.001
	Autophagy protein 5	CGI_10018604	1.93	<0.001
Adapter protein for E3	Brain tumor protein	CGI_10009245	3.13	<0.001
	BTB/POZ domain-containing protein 6	CGI_10025781	1.19	0.008
De-ubiquitinase	Ubiquitin carboxyl-terminal hydrolase	CGI_10008715	1.41	0.006
	Ubiquitin carboxyl-terminal hydrolase 27	CGI_10005873	1.81	<0.001
	Ubiquitin carboxyl-terminal hydrolase 4	CGI_10005143	3.22	0.001
Others	B-cell receptor-associated protein 31	CGI_10002335	1.53	0.005
	X-box-binding protein 1	CGI_10005445	1.17	0.002
	Mitotic spindle assembly checkpoint protein	CGI_10019832	1.33	<0.001

Table S7: Changes in the transcriptional expression of the *C. gigas* protein processes related genes of R29°C compared to R21°C transcriptomic response, during the early response to OsHV-1 infection (LFC: Log Fold Change).

Table S8. Transcripts related to metabolic process differentially expressed at 12 hpc.

Biological process	Gene name	CGI	LFC	P-value
Carbohydrates catabolism	α -glucosidase	CGI_10019976	-1.55	0.001
	β -galactosidase	CGI_10013358	-1.00	0.008
	Aldose-1- epimerase	CGI_10002487	-1.48	0.008
	Aldose-1- epimerase	CGI_10013973	-1.44	0.007
Glycolyse	glyceraldehyde 3 P-dehydrogénase	CGI_10010974	-1.01	0.007
	3-D phosphoglycerate kinase	CGI_10019050	-1.46	<0.001
	Hexokinase type 2	CGI_10023886	-1.43	<0.001
	Ketohexokinase	CGI_10024334	-1.83	<0.001
Neoglucogénèse	Phosphoenolpyruvate carboxykinase [GTP]	CGI_10014916	-1.16	0.004
Pentose-phosphate shunt, oxidative branch	Glucose 6-P Dehydrogenase	CGI_10011948	-1.57	0.003
	6-P Gluconolactonase	CGI_10002865	-2.70	<0.001
	6-phosphogluconate dehydrogenase, decarboxylating	CGI_10026515	-1.95	<0.001
Lipid metabolism	Fatty acid synthase	CGI_10020387	-2.46	<0.001
	1-Acylglycerol-3-Phosphate O-Acyltransferase	CGI_10021268	-2.11	0.002
	Acetyl-coA acetyl transferase	CGI_10015045	-2.53	<0.001
Triglycerides	Diacylglycerol O-Acyltransferases	CGI_10018485	-3.38	<0.001
	Pancreatic lipase-related protein 2	CGI_10014664	-1.19	0.007
	Pancreatic triacylglycerol lipase	CGI_10003345	-1.18	0.002
	Pancreatic triacylglycerol lipase	CGI_10023931	-1.05	0.009
Cholesterol metabolic process	Sortilin-related receptor	CGI_10003883	-2.11	0.002
	Sortilin-related receptor	CGI_10004946	-1.31	<0.001
	Niemann-Pick C1 protein	CGI_10006575	-2.49	<0.001
	Niemann-Pick C2 protein	CGI_10010548	-6.96	<0.001
	Blast: insulin-induced protein	CGI_10015540	-3.29	<0.001
Retinol metabolism	Retinol dehydrogenase 11	CGI_10012632	-1.73	0.001
	Beta,beta-carotene 15,15'-monooxygenase	CGI_10019019	-1.42	0.003
	Cytochrome P450 2J6	CGI_10022128	-1.54	0.002
	Beta,beta-carotene 15,15'-monooxygenase	CGI_10026077	-1.39	0.009
	Retinal dehydrogenase 1 D9	CGI_10026868	-1.44	0.047
Metabolites transport	Sodium/glucose cotransporter 4	CGI_10011683	-2.03	0.003
	Sodium-coupled monocarboxylate transporter	CGI_10003941	-1.65	0.003
	Monocarboxylate transporter 12	CGI_10011575	-1.17	0.005
	Monocarboxylate transporter 2	CGI_10012587	-1.22	0.009
	Monocarboxylate transporter 7	CGI_10026270	-1.98	0.002
	Monocarboxylate transporter 9	CGI_10018848	-1.43	<0.001
Transcription/translation	Uracil phosphoribosyltransferase	CGI_10027611	-3.30	<0.001
	DNA replication licensing factor mcm4	CGI_10015825	-2.40	0.004
	Double-stranded RNA-specific adenosine deaminase	CGI_10012998	-1.10	0.006
	Peptidyl-prolyl cis-trans isomerase	CGI_10027352	-2.10	0.010

	Pre-mRNA-processing-splicing factor 8	CGI_10009423	-3.07	0.001
	Putative tyrosyl-tRNA synthetase, mitochondrial	CGI_10019167	-1.25	0.005
	rRNA-processing protein FCF1-like protein	CGI_10000030	-1.63	0.005
	Peptidyl-tRNA hydrolase 2, mitochondrial	CGI_10024491	-2.01	0.001
	Peptidyl-prolyl cis-trans isomerase	CGI_10023850	-2.22	0.007
	Peptidyl-prolyl cis-trans isomerase 6	CGI_10022249	-1.60	0.002
	Poly [ADP-ribose] polymerase 14	CGI_10012563	-1.90	0.001
Amino-acids anabolism	Pyrroline 5 carboxylate reductase	CGI_10010949	-2.09	<0.001
	Glutamate decarboxylase	CGI_10013951	-4.53	<0.001
	Aminobutyrate transaminase	CGI_10027541	-1.80	0.009
Amino-acids catabolism	Succinate semialdehyde dehydrogénase	CGI_10008392	-1.36	<0.001
	Methylcrotonyl CoA carboxylase	CGI_10023847	-1.86	<0.001
	L-Serine dehydrogenase	CGI_10008600	-1.25	0.002
	Fumaryl-acetoacetase	CGI_10006585	-1.59	<0.001
	S-adenosylmethionine synthase	CGI_10006000	-1.33	0.0020

Table S9: Changes in the transcriptional expression of the *C. gigas* metabolism processes related genes of R29°C compared to R21°C transcriptomic response, during the early response to OsHV-1 infection (LFC: Log Fold Change).